JOURNAL OF MATERIALS SCIENCE **33** (1998) 5229–5235

The manufacture and characterisation of single phase magnetite and haematite aligned fibres from an aqueous sol-gel process

R. C. PULLAR, D. R. PYKE, M. D. TAYLOR, A. K. BHATTACHARYA*
Centre for Catalytic Systems and Materials Engineering, Department of Engineering, University of Warwick, Coventry CV4 7AL, UK
E-mail: r.c.pullar@warwick.ac.uk

A stable iron(III)hydroxide sol was produced, spun as a gel fibre and collected as an aligned tow blanket. The alignment of the fibre was found to be 88.8% within $\pm 20^\circ$ of the axis of alignment, comparable to that of some commercially developed ceramic fibres. Heating in air at a temperature of 250 °C for 1 hour yielded single phase haematite fibres, and these were characterised by X-ray diffraction and electron microscopy. Upon reduction of the gel fibre in 5% H_2 in N_2 at 350 °C for 1 hour, single phase magnetite was obtained and characterised by X-ray diffraction, infrared and Mössbauer spectroscopy. The morphology of the fibre was studied, and it was found that the transformation to magnetite was accomplished with no compromise of integrity of the fibre or its alignment, although there was an accompanying change in microstructure. The strain to break of the magnetite fibres was measured to be of a least 0.6%, and this compares well with some commercial fibres.

1. Introduction

Magnetite, historically named lodestone, was the earliest magnetic material known to man, but ironically it is now considered as a soft magnet, and it is therefore not used in applications requiring permanency. However, it does possess interesting and useful conductive and piezoelectric properties.

Fe_3O_4 is a cubic ferrite with an inverse spinel structure, where the Fe^{3+} ions share equally the tetrahedral and octahedral sites, thus cancelling each other out and leaving only the spin of the Fe^{2+} ions in the remainder of the octahedral sites to contribute to the magnetic moment [1]. Because the bi- and trivalent ions share the octahedral sites exchange can occur between them resulting in a flow of current, and this makes magnetite an electrical conductor, with a conductivity of 250 Ω^{-1} cm^{-1} at room temperature [2]. Magnetite has a saturation magnetisation of 480 G at 20 °C, and the Curie point is at 585 °C, and it is unusual in having a negative anisotropy and a positive magnetorestriction [3, 4]. Despite a high coercivity magnetite is too unstable for common use as a recording medium and it cannot be used at high frequencies due to eddy current losses caused by its relatively high conductivity [5].

Fe_3O_4 has an unusual magnetic permeability which not only increases with temperature up to the Curie point but which also has a second peak at −154 °C. This is the Verwey transition [6], a zero point in crystal anisotropy below which the structure changes from cubic to orthorhombic with a preferred direction of magnetisation [7]. A consequence of this is an increase in resistivity due to the electron delocalisation effect being inhibited as more order is induced in the ions. Any non stoichiometric Fe^{3+} ions will reduce this effect and lower the temperature at which it occurs, as well as reducing the conductivity above the Verwey transformation. Above the Curie temperature magnetite also acts as a semiconductor [2].

Reduction of Haematite, α-Fe_2O_3, at 400 °C in an air-free reductive atmosphere has produced magnetite [8], although care must be taken as magnetic will oxidise back to maghemite (γ-Fe_2O_3) or haematite if heated in air or if the particles exceed 300 nm, and particles below 6 nm are paramagnetic instead of ferrimagnetic at room temperature [9]. Haematite is usually formed as a precursor of magnetite, but the preparation of haematite fibres as a material in their own right is also reported in this publication.

The production of magnetite as a fibre in an aligned form would enable the product to be incorporated into a composite matrix, opening up a new area of novel materials and applications exploiting the useful piezomagnetic properties and electrical conductivity of this material.

2. Experimental

2.1. Preparative methods

All chemicals and solvents used were commercially available ACS grade.

* Author to whom all correspondence should be addressed.

2.1.1. Sol preparation

17.46 g (0.0433 M) of iron(III)nitrate nonahydrate was dissolved in 25 ml of distilled water, and cooled in an ice bath. 60 ml of a solution of 4% NH_3 in distilled water was also cooled in ice. This was then added to the iron chloride solution over 15 minutes, whilst the mixture was still cooled in an ice bath and stirred at 400 RPM, until the solution had reached a pH of 5. The resulting thick brown precipitate of iron(III)hydroxide was filtered and washed with 4×50 ml of distilled water, also adjusted to pH 5, and the weight of the washed precipitate cake was 37.26 g (6.49% Fe by weight). The hydroxide was then peptised with concentrated nitric acid (0.54 ml, 0.0087 M) in a ratio of iron to acid of 5 : 1 which was added to 20 ml of distilled water. After addition the cake and acid were mixed at room temperature and atmospheric pressure for one minute, after which the digestion was continued on a rotary evaporator under a vacuum of 95 kPa and at a temperature of 35 °C. All of the hydroxide had been digested within half an hour and a sol had formed, but the sol continued to peptise for up to 24 hours, after which time there was no further significant decrease in the average sol particle size. The resulting sol had a concentration of 10.11% Fe by weight (0.9462 M l^{-1}).

2.1.2. Fibre preparation

After filtering through a 0.7 μm filter and further concentration to over 20% Fe by weight, the iron sol was rendered spinnable by the addition of a polyethylene oxide (Aldrich, $M_W = 400{,}000$) spinning aid, at a level of 3% by weight to iron oxide. The spinning solution viscosity was about 3 poise, as measured on a paint cone-and-plate viscometer at 1000 s^{-1}. The fibres were produced by a modified proprietary blow spinning process [10, 11] in which the spinning solution is extruded through a row of holes on either side of which impinge parallel jets of humidified attenuating air at near ambient temperature. The fibres were drawn by these high velocity primary slit jets at a rate of 10 ms^{-1}, and gelled by mixing in secondary air at 110 °C. The fibre/air mixture passed down a short diverging section into a parallel duct to be collected on a rotating drum as an aligned blanket. After collection the fibres were removed from the drum and stored in a circulating oven at 110 °C to await subsequent heat treatment.

2.1.3. Heat treatments of fibres

The gel fibres were fired in air for 1 hour at temperatures of up to 400 °C to form haematite fibres.

The gel fibres were fired under two different regimes to investigate their transformation into magnetite. In both cases however, the reduction step was carried out under a flowing atmosphere of 5% H_2 in N_2 at a flow rate of 200 cm^3 min^{-1}, in a tube furnace of 200 cm^3 volume which had been previously flushed with this mixture for half an hour. The fibres were also allowed to cool to room temperature under this mixture to prevent any re-oxidation and subsequent loss of the magnetite phase. The fibres were reduced in both alumina and platinum vessels, and neither had any apparent effect on the production of the magnetite phase. Unless otherwise stated, the firing time was 1 hour at the relevant temperature.

(i) The gel fibres were fired to 400 °C for 3 hours in air to remove the organic and nitrate components and then reduced in 5% H_2 in N_2 at temperatures between 250 and 450 °C.

(ii) The gel fibres were directly reduced under 5% H_2 in N_2, without a preliminary firing to remove the combustible products, at temperatures between 250 and 350 °C.

2.2. Characterisation

2.2.1. Photon correlation spectroscopy (PCS)

Particle size measurement of the sol above the 3 nm diameter range was measured on a Malvern Instruments Lo-C autosizer and series 7032 multi-8 correlator, using a 4 mw diode laser, 670 nm wavelength.

2.2.2. Assessment of fibre alignment

The fibres were collected as a blanket on a high speed rotor, in a manner similar to that used for "Safimax" alumina fibres [11], a development product which was an aligned blanket with 90% of the fibres within $\pm 10^\circ$ and all within $\pm 20^\circ$.

A small proportion of fibres cross the general alignment in this work and were estimated using an optical microscope at 40× magnification. The number of aligned fibres in a field was counted, together with the few crossing the alignment in the same field. Counts were made in up to 5 separate fields summing to several hundred generally aligned fibres and up to about 50 crossing the alignment.

The direction of the generally aligned fibres was analysed by traversing the electron micrographs with a protractor normal to the axis of alignment and measuring the deviations of at least 100 individual fibres. Two sets of data were taken from opposite sides of each micrograph.

2.2.3. X-ray powder diffraction (XRD) measurement

X-ray powder diffraction patterns of the samples treated at various temperatures were recorded in the region of $2\theta = 10$–80° with a scanning speed of 0.25°/min on a Philips PW1710 diffractometer using CuK_α radiation with a nickel filter. The Philips APD 1700 software was used to calculate the average size of the crystallites in a sample using the Scherrer equation:

$$D = K\lambda / h_{1/2} \cos\theta$$

where D = average size of the crystallites, K = Scherrer constant (0.9×57.3), λ = wavelength of radiation (1.5405), $h_{1/2}$ = peak width at half height and θ corresponds to the peak position.

2.2.4. Scanning electron microscopy (SEM)

The samples were coated with a nominal 6 nm Au/Pt in a Cressington 806 high resolution sputter coater. Scanning electron micrographs and analysis of the morphology of the samples was carried out on a Hitachi S-4000 FEG/SEM operating at 5 kV.

2.2.5. Surface area and porosity measurements

Surface areas and pore size distributions of the fibres were performed on a Micrometrics ASAP 2000 using N_2 as the adsorption gas. Samples were degassed at 300 °C for 6 hours prior to analysis.

2.2.6. Mössbauer spectroscopy

The *Mössbauer* spectra were recorded on a microprocessor controlled *Mössbauer* spectrometer at 298 K using a 25 m Ci Co^{57}-Rh source.

2.2.7. Infrared (IR) spectroscopy

IR spectra of the samples (prepared as KBr discs) were collected on a Galaxy 7020 FTIR spectrometer with an MCT detector. Spectra were recorded from 4000 to 400 cm^{-1} with a resolution of 4 cm^{-1} (32 scans).

2.2.8. Assessment of strain to break

A thin strip of blanket was glued on to a piece of sheet rubber with transparent double sided adhesive tape. The blanket was indented with stainless steel wires of reducing diameter from 1.2 down to 0.3 mm. The tape was carefully removed with the adhering fibre strip mounted on a glass slide and the lines of indentation examined under and optical microscope a 100× magnification.

3. Results and discussion

3.1. Iron(III)sol characterisation and stability

The stability and the resulting size of the sol particles was found to be sensitive to the preparative techniques and conditions employed, and PCS enabled us to measure and control the properties of the sol to a certain extent. The PCS data indicated that the average particle size of the iron(III) sol was 3.7 nm, with a polydispersity of 0.53 and a weight average of 2.8×10^4 amu. The volume distribution of the sol particles has a direct effect on the spinning process, and even a small number of large particles can severely impede or even nullify the spinnability of the sol. Therefore volume distribution is considered a more relevant measure than the Z average, and the volume average was found to be 4.7 nm, with an upper limit on particle size of 18 nm. The sol was found to be stable for a period of at least several months at a concentration of 11% Fe by weight, and was also stable at increased concentrations up to around 24% Fe, after which the sol begun to precipitate out causing a "mudding" of the sol.

3.2. Alignment of the fibres

The gel fibres were smooth and even in appearance, with straight and parallel sides and a diameter of between 2 and 10 μm, with a mean of 6 μm. The coarser fibres occurred because of coalescence of the parallel fibre streams during spinning, and some twinned fibres were also present. These twinned fibres can account for the wide variation in the diameter of the fibres, and the true average diameter of single fibres was estimated to be 3 μm. The problem of fibre coalescence will be removed with further development of the spinning process, resulting in fibres with a much smaller diameter deviation. The proprietary "Safimax" fibre process [11] was modified to allow the collection of more friable gel fibres; the collection rotor was operated well below, rather than slightly above the fibre generating velocity, and an open diverging rather than a converging air duct was used. As a result 5–10% of the fibre length crosses the general alignment because of looping on to the rotor. The remaining 90–95% are well aligned as can be seen in Fig. 1, which shows the aligned magnetite fibres. 88.8% of the fibres are within ±20° and 69.2% are within ±10° of the axis of alignment, and this compares reasonably well with "Safimax" alumina [11].

Both the protractor measurement on micrographs or direct measurement at 40× magnification are viewing deviations set into the fibre on a 1–2 mm scale. These cannot be removed by subsequent tensioning and can affect the packing into composites. The problems of looping and the slight waviness in the generally aligned fibres should be removed through further optimisation of the spinning process.

3.3. Fibre characterisation and morphology

3.3.1. Gel fibres heated in air

After heating in air for just 1 hour at 250 °C the gel fibres were found to have formed haematite, and the XRD pattern (Fig. 2) indicated that the α-Fe_2O_3 was present as a single phase product. This was supported by Mössbauer spectroscopy and IR spectroscopy, with a broad peak at 545 wavenumbers and a broad hump between 470 and 450 wavenumbers [12]. Using the XRD data the Scherrer equation yielded an average crystallite size of 17 nm. The surface and interior microstructure, as seen in Fig. 3, consisted of small spherical grains around 25 nm in diameter. The general fibre morphology of smooth, parallel sides was also retained, and the alignment of the fibres was unaffected. Porosity and surface area measurements of the haematite fibres gave an average pore diameter of 12 nm, a pore volume of 0.13 $cm^3\,g^{-1}$ and a surface area of 30 $m^2\,g^{-1}$, and the strain to break of the haematite fibres was estimated to be 0.3–0.4%. The sample was subjectively quite cohesive, and this combination of reasonable cohesion in the bulk combined with a poor response to a crushing or indentation test has been previously observed with catalytic grade "Saffil". We believe this is indicative of a porous structure, and this is confirmed by the porosity data above.

3.3.2. Gel fibres pre-fired to 400 °C in air prior to reduction

The XRD patterns for these fibres are shown in Fig. 4. After being heated at 400 °C for 3 hours the fibres were

Figure 1 Photograph demonstrating the alignment of magnetite fibres.

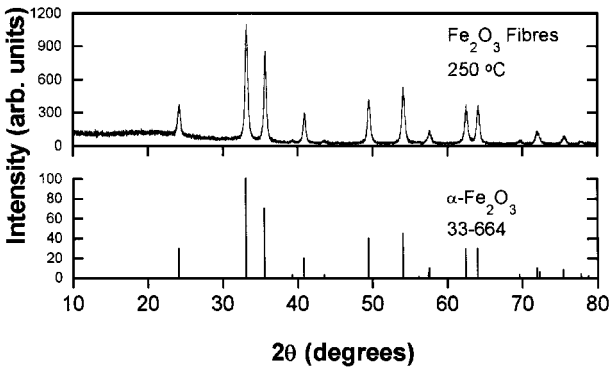

Figure 2 XRD pattern of gel fibres heated in air at 250 °C for 1 hour.

shown to have formed single phase haematite, α-Fe_2O_3, by XRD and IR spectroscopy, and the average crystallite size was given by the Scherrer equation as 22 nm. Upon heating in the reducing atmosphere at 250 °C and 300 °C the fibres remained as haematite (Fig. 4a) with no change in crystallite size. However, at 325 °C under reducing conditions magnetite had appeared as a second phase in association with haematite (Fig. 4b), in a ratio of about 2 : 3 haematite to magnetite. Even after longer firing periods of 15 hours haematite was still seen to be present as a minor phase, although the ratio had improved to 4 : 1 in favour of magnetite.

By 400 °C the haematite had become very much the minor phase (Fig. 4c), and the magnetite peaks were sufficiently well defined to obtain a crystallite size of 36 nm from the XRD data. Above this temperature the haematite persisted as a minor impurity, at the limit of detection by the XRD technique (Fig. 4d) but still enough to potentially compromise the electrical properties of the magnetite fibres. At 415 °C the average crystallite size for the magnetite had increased to 47 nm, but the trace of haematite was still present even with extended firing periods, this being confirmed by the Mössbauer spectra of the fibres. Therefore it appears extremely difficult to obtain pure magnetite by this method.

3.3.3. Direct reduction of gel fibres

The XRD patterns for these fibres are shown in Fig. 5. The fibres fired to 250 °C under a reducing atmosphere appeared to form single phase haematite from the XRD pattern (Fig. 5a) with a crystallite size of 18 nm, equal to that of the fibres which were fired to 250 °C in air. They also had a similar microstructure and grain size to the haematite fibres when examined under the SEM, and suffered no loss of alignment. The IR spectra also suggested pure haematite, having a broad peak at 545 wavenumbers and a broad hump between 470 and 450 wavenumbers [12], although a small magnetite peak could easily get swamped. However, the Mössbauer spectra indicated that even at this stage a trace of magnetite had started to form [13], and indeed by 275 °C magnetite had become the major phase in a ratio of 2 : 1.

The IR spectra of the fibres at 300 °C indicated that haematite had very much become a minor phase by this point, showing a strong magnetite peak at 564 wavenumbers which had a slight shoulder at 540 wavenumbers, and a much reduced broad hump still present between 470 and 450 wavenumbers. The XRD data agreed, and this sample at 300 °C resembled the pre-fired fibres after reduction at 400 °C (Fig. 5b). At this stage the magnetite fibres had an average crystallite size of 44 nm. The Mössbauer data also suggested a small percentage of haematite was still present [13].

After reduction at 350 °C for 1 hour the XRD pattern indicated that the fibres were single phase magnetite (Fig. 5c) with no trace of a haematite signal, and the Scherrer equation gave a crystallite size of 48 nm.

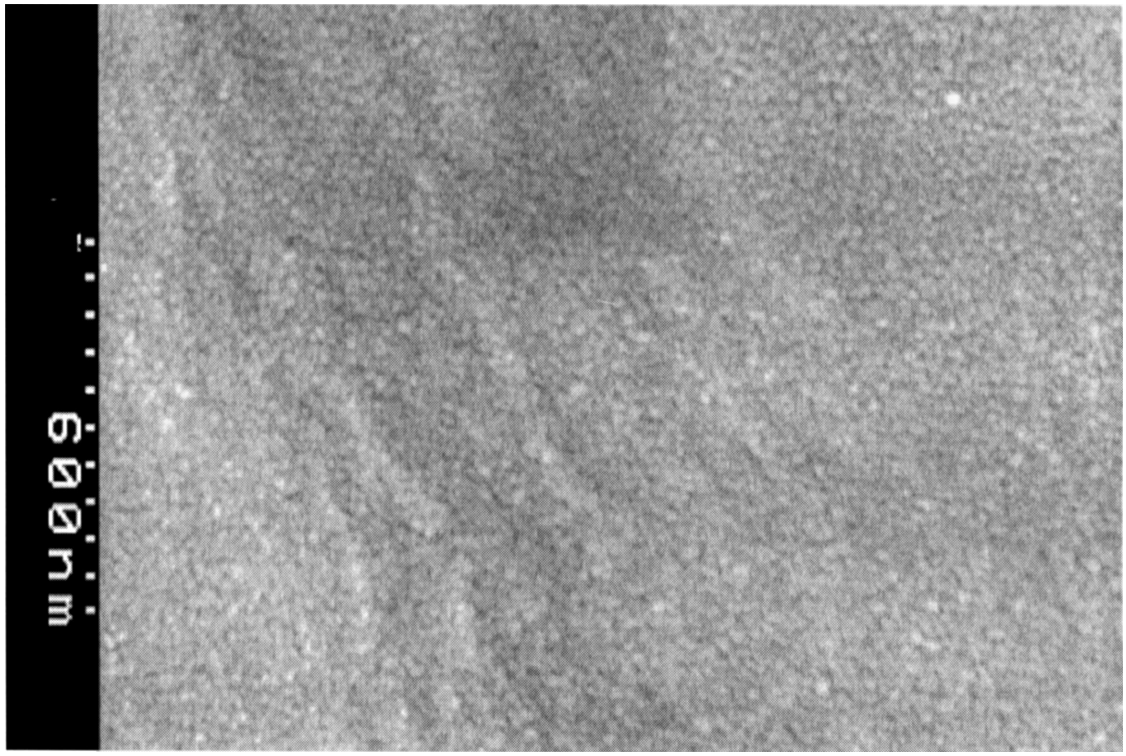

Figure 3 SEM micrograph of haematite fibres after being fired in air at 250 °C for 1 hour.

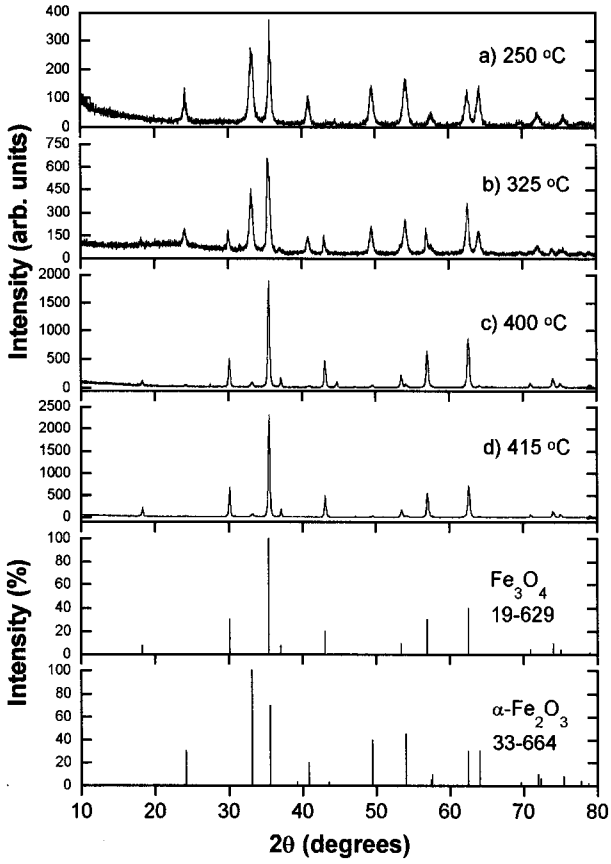

Figure 4 XRD patterns of gel fibres pre-fired in air at 400 °C and then reduced (a) 250 °C, (b) 325 °C, (c) 400 °C and (d) 415 °C for 1 hour.

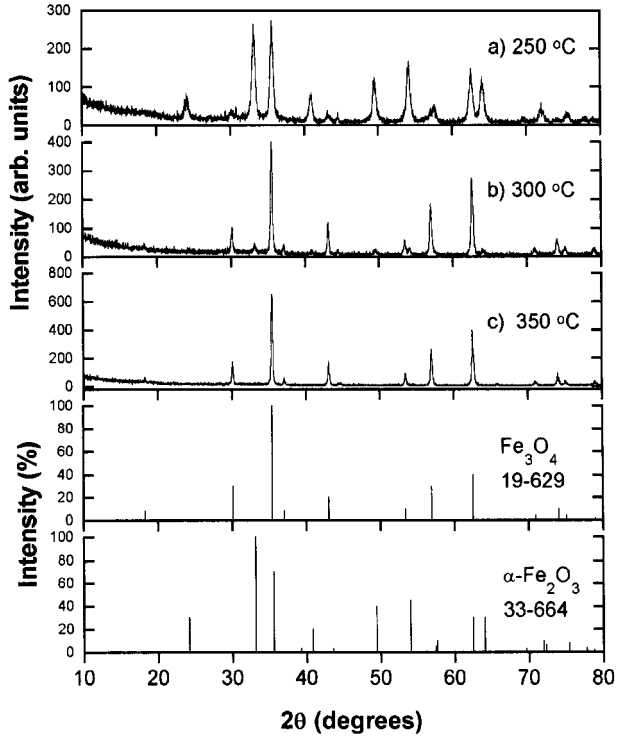

Figure 5 XRD patterns of gel fibres directly reduced at (a) 250 °C, (b) 300 °C and (c) 350 °C for 1 hour.

The IR spectra also indicated pure Fe_3O_4 with a strong peak at 570 wavenumbers, and the haematite peaks had vanished. Mössbauer spectroscopy is a more sensitive technique for detecting any traces of haematite, and it confirmed that these fibres were indeed single phase [13]. The Mössbauer spectrum for these fibres is reproduced in Fig. 6. The general morphology of individual fibres did not appear much changed from when they were haematite as they were still smooth and parallel sided, but the microstructure of the magnetite

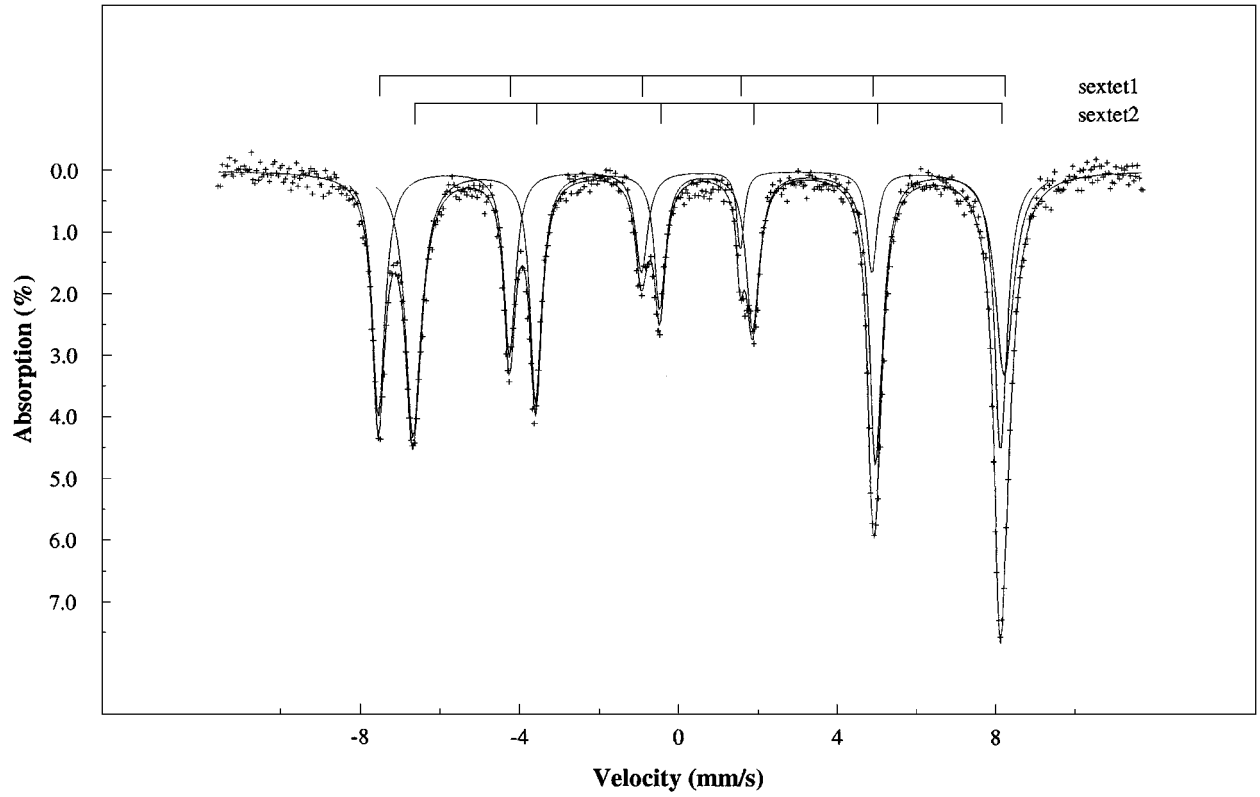

Figure 6 Mössbauer spectra of magnetite fibres directly reduced at 350 °C for 1 hour.

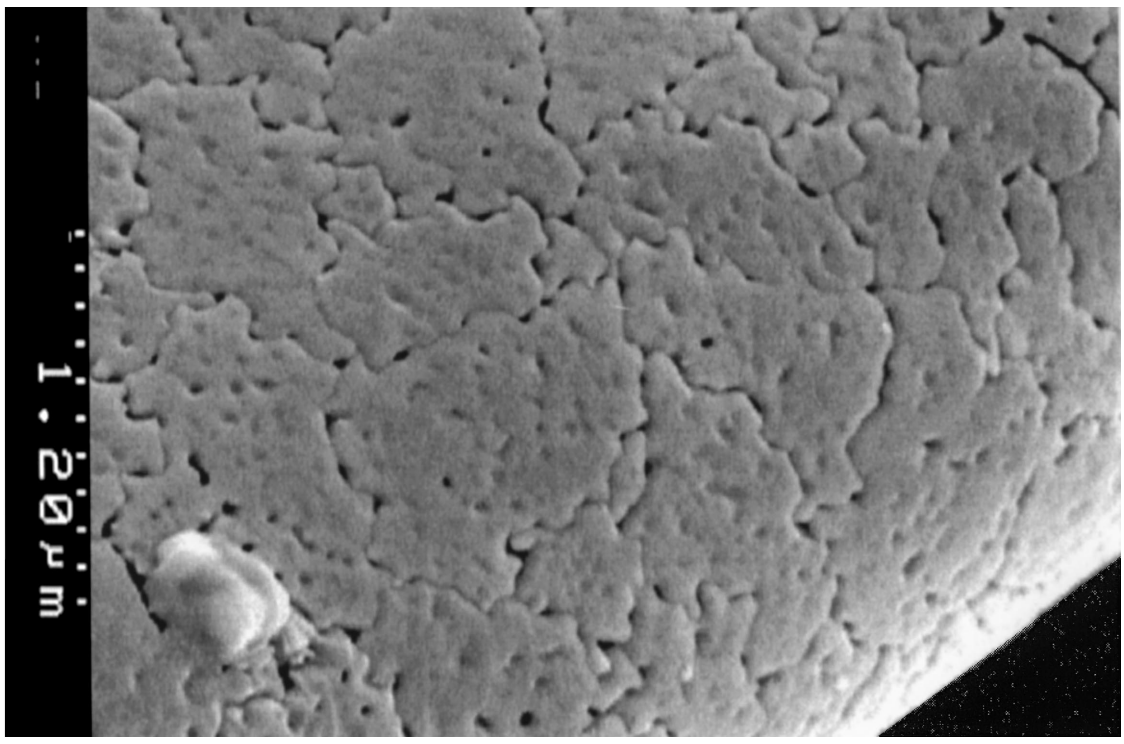

Figure 7 SEM micrograph of magnetite fibres directly reduced at 350 °C for 1 hour.

fibres was markedly different to that of the haematite fibres (Fig. 7). There were no discernible small grains as before, but instead the surface appeared to be pock-marked with dimples 50–100 nm in diameter, and it was also split into irregular islands between 0.2 and 1 μm in diameter, separated from one another by lines of "perforations", and in some cases cracks. This strongly resembles the irregular, wavy grain boundary phenomena which have occasionally been reported in other ceramic systems, such as $SrCaFe_2O_5$ [14]. These "perforations"

appeared to be pores 40–80 nm wide, and this concurs with the porosity and surface area measurements of the magnetite fibres, which gave an average pore diameter of 55 nm, a pore volume of 0.04 $cm^3\ g^{-1}$ and a surface area of 2.3 $m^2\ g^{-1}$.

In strain to break measurements on the magnetite fibres damage started to occur with a 1 mm wire with general breakage at 0.8 mm, indicating a strain to break given by the ratio of fibre to wire diameters, of the order of 0.6 to 0.75%. For strain to break to be of a least 0.6% is a promising result for a 6 μm fibre at the earliest stage of development, and compares well with commercial "Saffil" alumina which shows a strain to break of 0.7% at 3 μm.

4. Conclusions

A stable Iron(III)hydroxide sol was produced and gel fibres were then successfully spun from it and collected as an aligned tow blanket. These fibres had an alignment comparable with that of commercially available "Saffimax" ceramic fibres, and they maintained that degree of alignment when they were converted into magnetite or haematite.

It proved to be considerably easier to produce haematite than magnetite. The gel fibres formed single phase α-Fe_2O_3 when heated at only 250 °C for 1 hour in air, with a fine grain size of 25 nm. The fibres were found to have a quite porous structure which resulted in a mechanically weak fibre, with a strain to break of 0.3–0.4%.

It was discovered that if the Iron(III)hydroxide gel fibres were then heated at 250 °C in an atmosphere of 5% H_2 in N_2 for 1 hour they too transformed to haematite. With a further increase in temperature magnetite became the major phase at the expense of the haematite phase. At 350 °C in a reducing atmosphere for 1 hour the fibres consisted of the single magnetite phase. This change of phase was accompanied by a corresponding change in surface microstructure, although the overall morphology of the whole fibre remained largely unchanged. The magnetite fibres had a strain to break comparable to that of commercially available fibres.

If the gel fibres were firstly pre-fired at 400 °C in air to remove any combustible species, they form haematite similar to that formed at 250 °C. However, upon subsequent reductive firing it was found that single phase magnetite could not be obtained without the presence of traces of haematite as a minor impurity.

Acknowledgements

R. C. Pullar wishes to thank the Centre for Catalytic Systems and Materials Engineering for providing funding for his research associateship. Our thanks to A. G. Kinniburgh for surface area measurements, R. C. Reynolds for the XRD spectra and G. S. Walker for the IR spectra (all at the Centre for Catalytic Systems and Materials Engineering, Department of Engineering, University of Warwick) and Professor F. J. Berry for the Mössbauer analysis (Department of Chemistry, The Open University).

References

1. C. HECK, "Magnetic Materials and their Applications" (Butterworth and Co. Ltd., London, 1974).
2. S. KRUPICKA and P. NOVAK, *Ferromagnetic Materials*, p. 263.
3. D. J. CRAIK and R. S. TEBBLE, "Ferromagnetism and Ferromagnetic Domains" (North-Holland Publishing Company, Amsterdam, 1965) pp. 93–96.
4. J. SMIT and H. P. J. WIJN, "Ferrites" (Philips Technical Library, Eindhoven, 1959) p. 157.
5. J. P. JAKUBOVICS, "Magnetism and Magnetic Materials" (The Institute of Metals, Cambridge, 1994) p. 107.
6. E. J. W. VERWEY and P. W. HAAIJMAN, *Physica*. **8** (1941) 979–87.
7. L. R. BICKFORD, J. M. BROWNLOW and R. F. PENDYER, *Proc. IEE-B* **104** (1957) 238–244.
8. A. E. REGAZZONI, G. A. URRUTIA, M. A. BLESA and A. J. G. MAROTO, *J. Inorg. Nucl. Chem.* **43** (1981) 1489–1493.
9. R. M. CORNELL and U. SCHWERTMANN, "The Iron Oxides" (VCH, New York, 1996) p. 368.
10. M. J. MORTON, J. D. BIRCHALL and J. E. CASSIDY, (ICI) UK Patent 1360200 (1974).
11. M. H. STACEY and M. D. TAYLOR, (ICI) Eur. Patent 318203 (1987).
12. R. A. NYQUIST and R. O. KAGEL, "Infrared Spectra of Inorganic Compounds" (Academic Press, London, 1971).
13. E. MURAD and J. H. JOHNSTON, "MössBauer Spectroscopy Applied to Inorganic Chemistry," Vol 2, edited by G. Long (Plenum Publishing Corp., New York, 1987) pp. 2507–2582.
14. M. P. HARMER, H. M. CHAN and D. M. SMYTH, *Mater. Res. Soc. Symp. Proc.* (*Defect Prop. Process, High Technol. Nonmet. Mater.*) (1986) 125–134.

Received 4 September 1997
and accepted 14 September 1998